Journal of Applied Electrochemistry **30**: 1097–1102, 2000.

Effect of chromate additive on the kinetics and mechanism of skeletal copper formation

A.J. SMITH, L. MA, T. TRAN* and M.S. WAINWRIGHT
*School of Chemical Engineering & Industrial Chemistry, University of New South Wales, Sydney, Australia, 2052 (*author for correspondence)*

Received 7 December 1999; accepted in revised form 1 May 2000

Key words: chromium dopant, de-alloying, Raney®† copper catalysts, selective dissolution, structure

Abstract

The addition of chromate to the leach liquor for the preparation of skeletal copper increases and stabilizes the copper surface area and slows the leaching rate. The kinetics have been studied using a rotating disc electrode (RDE) at 269–293 K in 2–8 M NaOH and 0–0.1 M Na_2CrO_4. The rate of leaching was found to be constant with time, with an activation energy of 74 ± 7 kJ mol^{-1}. By monitoring the kinetics and free (mixed) corrosion potential, it was possible to elucidate the mechanistic effect of chromate causing the increased surface area. Chromate was found to deposit on the copper surface as chromium(III) oxide, hindering the leaching reaction as well as the dissolution/redeposition of copper, the main mechanism of structural formation/rearrangement for skeletal copper. This blocking of the surface resulted in a finer structure, with a corresponding larger surface area. It also stabilised the surface area by minimizing the rearrangement. The effect of chromate was found to reach a limit at around 0.03 M Na_2CrO_4.

List of symbols

A_{disc}	flat geometric surface area of the rotating alloy disc (m^2)
$\alpha_{H_2,Cu}$	transfer coefficient for H_2 evolution on Cu
E	actual potential (V)
$E^{\circ\prime}_{H_2}$	formal potential for the hydrogen evolution reaction (V)
F	faradaic constant (96 486 C mol^{-1})
$k^0_{H_2,Cu}$	standard rate constant for hydrogen evolution on pure copper
K	proportionality constant
k_d, k_r	rate constants for the leaching and rearrangement reactions, respectively
n_a	number of electrons transferred in the rate limiting step
R	gas constant (8.314 J mol^{-1} K^{-1})
$r_{L,0}$	initial ligament radius (m)
T	absolute temperature (K)
t	time (min)
x	rearrangement exponential

1. Introduction

Raney® copper, produced by the selective dissolution of aluminium from a copper–aluminium alloy, is an active hydrogenation catalyst [1–3]. In particular, Raney® copper is selective towards methanol synthesis from syn-gas [4–9]. Recently, it has been shown [10–12] that adding chromium to the system greatly increases the specific surface area of the catalyst, and hence specific activity, whilst also providing structural integrity. The exact way in which the chromium is able to increase the surface area of the copper and to stabilize it against rearrangement is the focus of this work. It is important to note that with the addition of an additive, the leached product is referred to as 'skeletal' to avoid infringement of the Raney® trademark.

A previous paper [13] described an electrochemical study for understanding the formation and rearrangement mechanisms of Raney® copper, produced by selectively dissolving aluminium from a $CuAl_2$ alloy. The main equation derived (Equation 1) related the free corrosion potential of the dissolving alloy (E) to time (t). Based on this equation, the slope of a plot of E against $\ln(t)$ gave a value for 'x' that corresponded to the mechanism of formation/rearrangement of the Raney® structure (x = 1 for viscous flow, 0.5 for dissolution/redeposition, 0.33 for volume diffusion, and 0.25 for surface diffusion). Equation 1 was derived on the basis of a constant aluminium leaching rate and a structure consisting of cylindrical ligaments [13].

† Raney® is a registered trademark of W.R. Grace & Co

$$E = \frac{RT(1-x)}{\alpha_{H_2,Cu} n_a F}\ln(t) - \frac{RT}{\alpha_{H_2,Cu} n_a F}\ln\left(\frac{3A_{disc}\dfrac{dAl^{3+}}{dt}k_r(1-x)}{2k^0_{H_2,Cu} r_{L,0} K k_d}\right) + E^{\circ'}_{H_2} \quad (1)$$

For the Raney® copper system (without additives), the main mechanism for the formation and subsequent rearrangement of the residue copper structure, upon selective leaching with hydroxide and in the absence of diffusion limitations, was found to be dissolution/redeposition of the copper, with diffusion playing a minor role [13]. The technique was not able to distinguish between surface and volume diffusion. Surface diffusion refers to the movement of atoms along an exposed surface whereas volume diffusion refers to atom movement within the bulk solid.

The previous paper on skeletal copper formation [13] made extensive use of a 'focussed ion beam' (FIB) for revealing the internal structure. A FIB works by focussing gallium ions onto the sample. At high beam currents, the ions sputter the sample where they are focussed, effectively milling into the solid. At low beam currents, there is still some sputtering occurring, especially with sensitive samples, however the sample is usually stable enough allowing imaging. Images are obtained using the backscattered electrons emitted when the ions hit the solid. The FIB allows samples to be milled then tilted, exposing the internal structure *in situ*.

The present paper is a continuation of previous work [13] and was conducted to: (i) investigate the effect of chromium on the leaching kinetics in the absence of diffusion limitations; (ii) understand how chromium causes a higher copper surface area; (iii) understand how chromium stabilizes the copper residue against rearrangement; and (iv) investigate how the chromium is incorporated into the copper structure.

Simultaneously to the present work, an independent study on the same system was undertaken using a different technique [14]. The study used small particles instead of large discs, and monitored the reaction rate by digesting and analysing the remaining alloy particles during the leaching. The data were fitted to a shrinking core model [15]. The results from this other study will be directly compared to the kinetic results from the current work before possible mechanisms are explored.

2. Experimental details

The precursor alloy for all experiments was supplied by Riverside Metal Industrial Pty Ltd and consisted of 52.17% w/w Al, remainder Cu. The alloy was re-cast into rods and quenched, ensuring homogeneity. The rods were machined to exactly 20.0 mm diameter, then cut using an abrasive cut-off wheel into discs about 3 mm thick. The discs were polished to 1 μm on one face using diamond grinding pads.

The structure of the leached alloy was examined using a FEI/Philips FIB (Focussed Ion Beam). Alloy discs were leached with 6 M NaOH + 0.025 M Na_2CrO_4 at 274 K overnight. After thorough washing in distilled water and then in alcohol, the samples were placed in a vacuum desiccator before transfer to the microscope.

The mechanism of copper rearrangement in the presence of chromium was studied using two rotating disc electrode (RDE) setups. The first setup was custom-made where the 20 mm alloy discs were held in a perspex holder, allowing the polished faces to freely dissolve in the leaching solution while their free corrosion potential was monitored against a Ag/AgCl reference electrode. The rate of reaction was followed by analysing the aluminium concentration in successive samples by ICP–AES. The second setup was a Pine Instruments MSR RDE, where a small rod of alloy or pure metal was imbedded in perspex which connected to the rotating shaft, and the bottom face could be polished to give a circular cross section. A BAS CV-27 voltammograph was used to control the potential and measure the current. For both setups, the leaching solution was sodium chromate dissolved in sodium hydroxide, each at various concentrations as noted in the results.

All measurements in this work are within a maximum of 10% error, and all potentials are reported against a Ag/AgCl reference electrode.

3. Results and discussion

3.1. *Structure*

Figure 1 shows the structure of skeletal copper produced by leaching in 6 M NaOH without additives, while Figure 2 shows skeletal copper leached in 6 M NaOH in the presence of 0.025 M Na_2CrO_4. The addition of chromate caused the leached structure to be much finer, explaining the observed increased surface area [11]. The shape of the structure, a uniform three-dimensional network, remained the same.

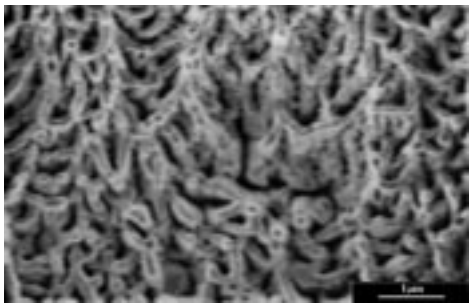

Fig. 1. FIB image of Raney® copper leached with 6 M NaOH at 274 K (no additives) [13].

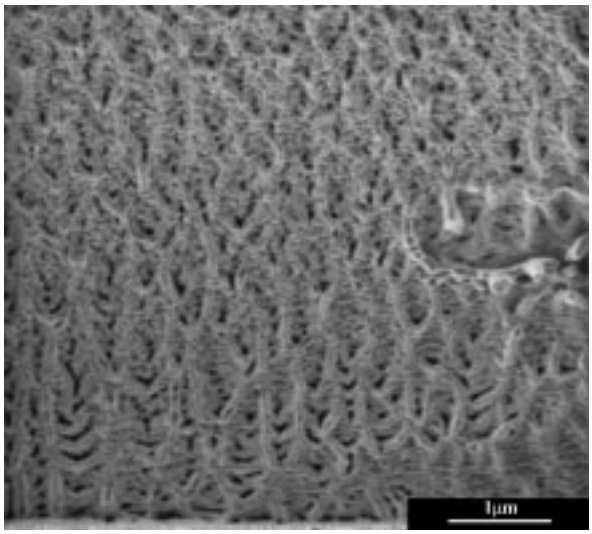

Fig. 2. FIB image of skeletal copper leached with 6 M NaOH + 0.025 M Na_2CrO_4 at 274 K. Magnification identical to image in Figure 1.

3.2. *Leaching kinetics*

The leaching reaction, in the absence of diffusion limitations, showed a constant leaching rate within the concentration range of 0.005–0.1 M sodium chromate and the temperature range 269–293 K. Figure 3 shows this constant leaching rate for different temperatures. The constant leaching rate was also seen in the system without additives [13], although the overall leaching rate was slower in the presence of chromate. Ma et al. [14] also found a constant initial leaching rate, however this soon gave way to a decreasing leaching rate with time as the small particles became fully leached. The effect of chromate concentration on the rate is shown in Figure 4, which gives an approximately logarithmic relation, similar to that found independently by Ma et al. [14].

The data in Figure 3 can be plotted to fit the Arrhenius equation (Figure 5), giving an activation energy of 74 kJ mol^{-1}. This is in agreement with Ma et al. [14], who found an activation energy of 72 kJ mol^{-1} for the same system using a different technique, and compares to 69 kJ mol^{-1} for the system without additives [13].

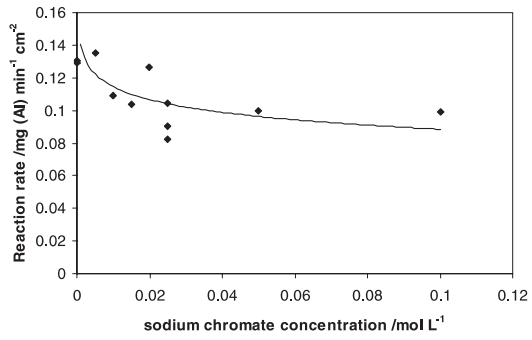

Fig. 4. Effect of chromate concentration on rate of leaching (6 M NaOH, 274 K).

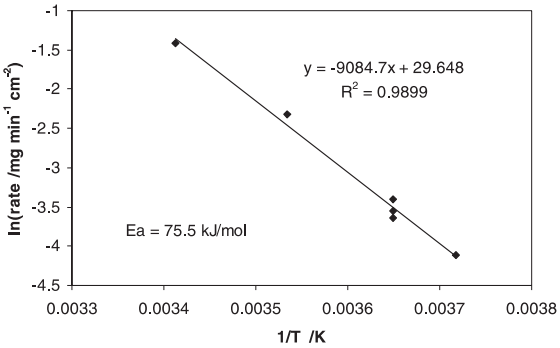

Fig. 5. Arrhenius plot for the leaching reaction (6 M NaOH + 0.025 M Na_2CrO_4). From the slope, the activation energy is 73.6 kJ mol^{-1}.

There was no obvious relation between leaching rate and hydroxide concentration (Figure 6), however the same convex shape to the points was present in the system without additives [13]. Ma et al. [14] observed that the leaching rate increases slightly with increasing hydroxide concentration up to about 6 mol L^{-1}, then decreases with higher hydroxide concentrations. This corresponds to the convex shape in Figure 6.

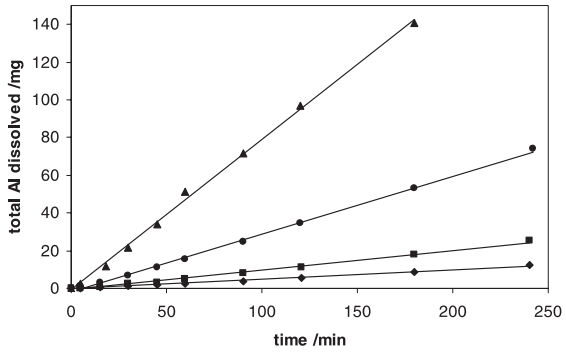

Fig. 3. Rate of leaching at various temperatures in 6 M NaOH + 0.025 M Na_2CrO4. Key: (◆) 269 K, (■;) 274 K, (●) 283 K and (▲) 293 K.

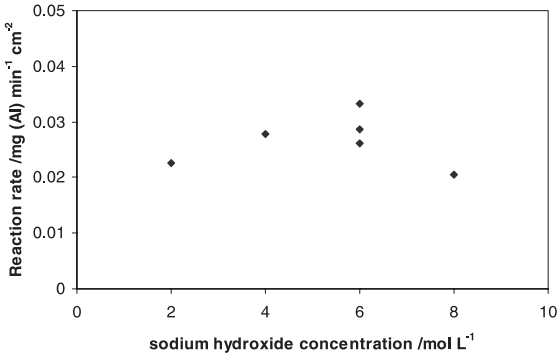

Fig. 6. Hydroxide concentration has little affect on the leaching rate. Data from 274 K and 0.025 M Na_2CrO_4.

3.3. *Mechanism theory without additives and effect of chromate*

Equation 1 was derived for a system showing a constant leaching rate and a hydrogen evolution current equal to the aluminium dissolution current. For now it will be assumed that the chromate does not significantly interfere with the equality between the hydrogen and aluminium currents; this will be verified later in the discussion. With this assumption, and since the leaching rate is constant in the presence of chromate (Figure 3), Equation 1 can also be used for the chromate system. Thus a plot of E against $\ln(t)$ will give a value for 'x' which corresponds to the mechanism of formation and rearrangement of the de-alloyed residue. Figure 7 shows plots of E against $\ln(t)$ for selected data, with linearity proving compliance with Equation 1.

The value for x in the presence of chromate was found to be around 0.40, slightly less than the 0.50 for the system without additives [13]. This demonstrates that, compared to no additive, there is a greater proportion of diffusion to dissolution/redeposition in the mechanism. This difference in proportion must correspond to an overall reduction in the amount of dissolution/redeposition, since this would mean less rearrangement and hence a greater surface area, which is observed when chromate is added to the system.

The value for x, and hence the mechanism, depends on both temperature and chromate concentration. Figure 8 shows that increasing the temperature causes x to decrease, corresponding to a greater proportion of diffusion. Figure 9 shows overall that increasing the chromate concentration also decreases x. However very small chromate additions actually have the opposite effect: increasing the x value. Larger chromate additions show a 'saturation' affect towards the lowering of x, with the reduction in x decreasing with increasing chromate concentration. The effect of temperature and chromate concentration on the mechanism will be explained below.

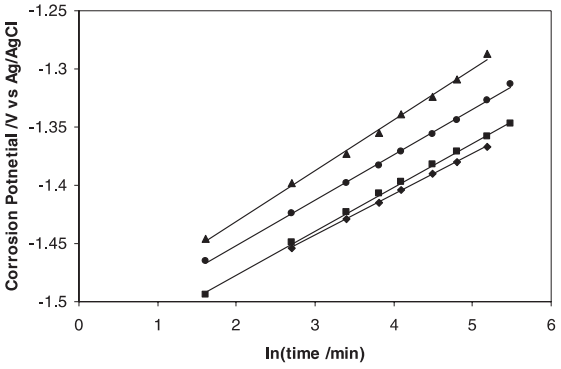

Fig. 7. Corrosion potential against the logarithm of time. Linearity verifies compliance of the system to Equation 1. Key: (◆) 269 K, (■) 274 K, (●) 283 K and (▲) 293 K.

3.4. *The chromate mechanism*

The Evans diagram in Figure 10 suggests that Cr(VI) will be reduced to Cr(III) at the free corrosion potential of leaching of $CuAl_2$ (around −1.3 to −1.5 V vs Ag/AgCl). Ma et al. [16] confirmed this by detecting chromium(III) oxide on the surface of skeletal copper when the leachant was doped with chromate. From the Pourbaix diagram [17], chromium(III) oxide will not easily re-oxidize at the corrosion potential of leaching. However, it is slightly soluble at high pH, and so may slowly redissolve as chromite (CrO_2^-) as Ma et al. have

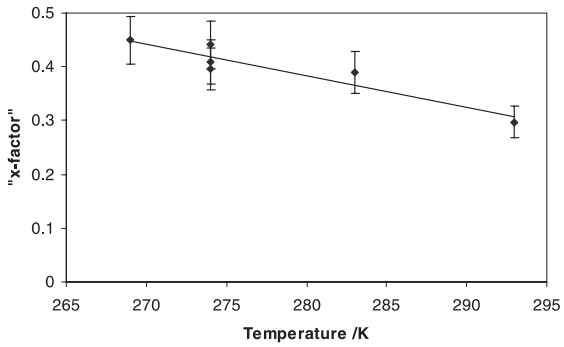

Fig. 8. 'x-factor' against temperature (6 M NaOH + 0.025 M Na_2CrO_4).

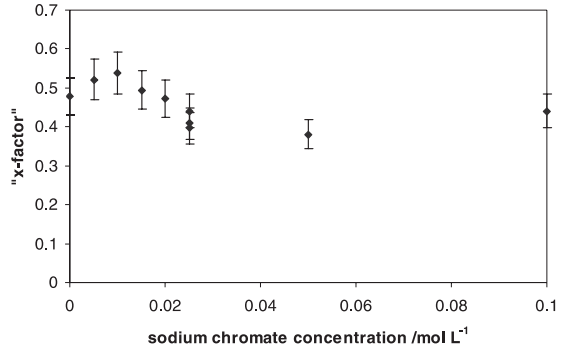

Fig. 9. 'x-factor' against chromate concentration (6 M NaOH, 274 K).

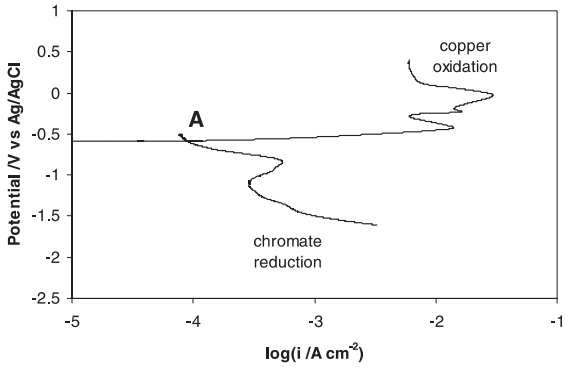

Fig. 10. Evans diagram (E vs $\ln(i)$). Scanning positively for Cu oxidation, scanning negatively for CrO_4^{2-} reduction. 6 M NaOH + 0.025 M Na_2CrO4, 274 K, copper electrode, 0.015 V s^{-1}, 2500 rpm. Intersection 'A' represents the oxidation of copper by chromate ions (low current density of about 10^{-4} A cm^{-2}).

found [14]. Figure 10 also shows that chromate, although thermodynamically capable [17], will not greatly oxidize bulk copper under the conditions of leaching due to kinetic hindrance (the reaction is extremely slow). Point A in Figure 10 is the intersection of the chromate reduction reaction and the copper oxidation reaction, indicating the low oxidation current of the order of 10^{-4} A cm^{-2}.

For chromate reduction electrons are required which can only originate from the aluminium ionisation. According to Ma et al. [14], there is at least a 100-fold difference above the stoichiometric amount between the moles of aluminium ionised and the moles of chromium deposited. This indicates that the chromate does not significantly interfere with the equality between aluminium ionisation and hydrogen evolution. This verifies the previous assumption and indicates that Equation 1 holds.

By depositing on the unleached alloy surface, the chromium(III) oxide hinders the dissolution of aluminium, slowing the leaching rate (as observed in Figure 4). This blocking effect would display the 'saturation' phenomenon shown in Figure 4. By also depositing on the copper residue, the chromium(III) oxide hinders the dissolution of copper, the primary structural rearrangement mechanism. This is seen as a fall in the value of x with increasing chromate ion concentration. Reducing rearrangement allows for a higher copper surface area to form and be maintained.

The rate of deposition of chromium(III) oxide increases with increasing temperature [14]. This corresponds to extra blocking of the copper surface, hindering the dissolution/redeposition of the copper, thus resulting in the lower observed x-value at higher temperatures (Figure 8).

The blocking effect of the chromium(III) oxide, preventing the dissolution of the copper, and hence rearrangement by that mechanism, is only one of three main mechanisms that could theoretically operative to give higher copper surface areas. A second mechanism might involve chromium(III) oxide depositing on the surface and acting as a nucleation source for the copper to deposit on once it has dissolved (during the dissolution/redeposition mechanism) [19, 20]. This nucleation would enhance the fineness of the structure and hence surface area. A third possible mechanism for increasing the surface area of the copper, proposed for general de-alloying [21, 22], states that the rate of rearrangement of a de-alloyed residue is proportional to the de-alloying rate, due to the number of defects formed during the de-alloying. This 'defect' mechanism suggests that because the chromate slows the leaching rate, there will be fewer defects in the copper residue. Hence, the rate of rearrangement of the copper will be slower, thus giving a higher surface area.

Of all three possible mechanisms, only the blocking mechanism is actually capable of altering the value of x, the proportion of dissolution to diffusion of copper, therefore this particular mechanism must be operative. To test whether the deposited oxide acts as a nucleation source for enhancing the fineness of the copper structure, the presence of chromium needs to be detected inside the copper ligaments. Work to locate additives within the skeletal copper structure will be published separately [23]. Briefly, elemental mapping using a STEM (scanning transmission electron microscope) showed chromium located on the outside of the copper ligaments. This indicates the nucleation mechanism is not active.

The defect mechanism can be tested with current data. From Equation 1, the intercept of E against $\ln(t)$ is

$$int = -\frac{RT}{\alpha_{H_2,Cu} n_a F} \times \ln\left(\frac{3A_{disc}\frac{dAl^{3+}}{dt}k_r(1-x)}{2k^0_{H_2,Cu} r_{L,0} K k_d}\right) + E^{o'}_{H_2} \quad (2)$$

However, since the leaching rate is constant, $dAl^{3+}/dt = k_d$, and so these two cancel giving

$$int = -\frac{RT}{\alpha_{H_2,Cu} n_a F}\ln\left(\frac{3A_{disc}k_r(1-x)}{2k^0_{H_2,Cu} r_{L,0} K}\right) + E^{o'}_{H_2} \quad (3)$$

According to the defect mechanism $k_r \propto k_d$, and since $int \propto \ln(k_r)$ (Equation 3), then int must be proportional to $\ln(k_d)$ for this mechanism to be operative. By taking data points from various chromate concentrations, different k_d's exist without changing the temperature. A plot of int (from E vs $\ln(t)$) against $\ln(k_d)$ for different chromate concentrations is given in Figure 11. There is no obvious relation in this graph so the defect mechanism can be regarded as not operative, or only a very minor player in the mechanism of forming a higher surface area in the current system.

4. Conclusions

Addition of chromate slows the leaching rate; however the rate remains constant with time. The leached structure is much finer than in the absence of chromate.

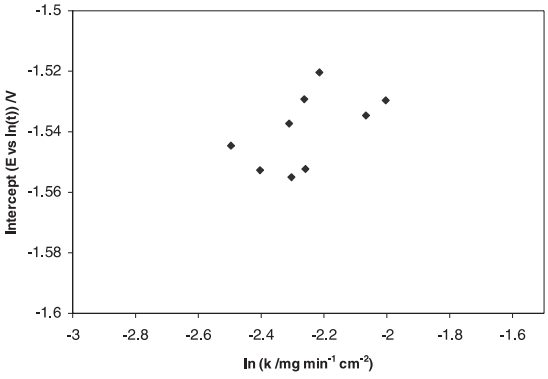

Fig. 11. Plot of the *intercept* of [E vs $\ln(t)$] against ln(leaching rate) for various amounts of chromate additions.

The effect of chromate on the mechanism of formation/rearrangement of skeletal copper is to decrease the amount of dissolution/redeposition of copper by depositing as chromium(III) oxide on the surface. This reduction in rearrangement leaves a much finer structure (higher surface area of copper) compared to un-doped skeletal copper. The deposited oxide also serves to stabilize the copper structure and is the cause of the slower leaching rate. The effect of chromate reaches a limit at about 0.03 M Na_2CrO_4.

Acknowledgements

Financial support from the Australian Research Council is gratefully acknowledged. AJS acknowledges receipt of an Australian Postgraduate Award. The authors would also like to thank A/Prof. Paul Munroe and Ms Viera Piegerova, from the Electron Microscope Unit at UNSW, for their invaluable assistance in obtaining the micrographs. Also, thanks to Brian Cooper for the casting work and Gautam Chattopadhyay for assistance with the ICP analysis.

References

1. M. Raney, *Ind. Eng. Chem.* **32**(9) (1940) 1199.
2. B.V. Aller, *J. Appl. Chem.* **8** (1958) 492.
3. J.A. Stanfield and P.E. Robbins, 'Raney copper catalysts' *in* Proc. 2nd Int. Cong. Catal., Paris (1960), pp. 2579–2599.
4. M.S. Wainwright, 'Raney copper – A potential methanol synthesis catalyst' *in Alcohol Fuels*, Sydney, 9–11 Aug. (1978), p. 8-1.
5. W.L. Marsden, M.S. Wainwright and J.B. Friedrich, *Ind. Eng. Chem. Prod. Res. Dev.* **19**(4) (1980) 551.
6. J.B. Friedrich, D.J. Young and M.S. Wainwright, *J. Catal.* **80** (1983) 1.
7. J.B. Friedrich, D.J. Young and M.S. Wainwright, *J. Catal.* **80** (1983) 14.
8. H.E. Curry-Hyde, D.J. Young and M.S. Wainwright, *Appl. Catal.* **29** (1987) 31.
9. M.S. Wainwright and D.L. Trimm, *Catal. Today* **23** (1995) 29.
10. L. Ma, D.L. Trimm and M.S. Wainwright, Promoted Skeletal Copper Catalysts for Methanol Synthesis *in* 'Advances of Alcohol Fuels in the World', Beijing, China, 21–24 Sept. (1998), pp. 1–7.
11. L. Ma and M.S. Wainwright, *Appl. Catal. A* **187** (1999) 89.
12. L. Ma, D.L. Trimm and M.S. Wainwright, *Topics in Catalysis* **8** (1999) 271.
13. A.J. Smith, T. Tran and M.S. Wainwright, *J. Appl. Electrochem.* **29**(9) (1999) 1085.
14. L. Ma, A.J. Smith, T. Tran and M.S. Wainwright, *Chem. Eng. Process.* (submitted 1999).
15. O. Levenspiel, 'Chemical Reaction Engineering', 2nd edn (J. Wiley & Sons, Singapore, 1972), p. 372.
16. L. Ma, B. Gong and M.S. Wainwright, 'Cr_2O_3 promoted skeletal Cu catalysts for the reactions of methanol steam reforming and water gas shift' *in* 2nd Asia-Pacific Congress on Catalysis, Sydney, Australia, 31 Jan.–2 Feb. (2000), (submitted 1999).
17. M. Pourbaix, 'Atlas of Electrochemical Equilibria in Aqueous Solutions', National Association of Corrosion Engineers, Houston, Texas, USA (1974) Sections 10.1 and 14.1.
18. K. Sieradzki, *J. Electrochem. Soc.* **140**(10) (1993) 2868.
19. M.M. Kalina, A.B. Fasman and V.N. Ermolaev, *Kinet. Katal.* **21**(3) (1980) 813.
20. M.M. Kalina, A.B. Fasman and V.N. Ermolaev, *Deposited Doc., VINITI* **1022–80** (1980) pp. 15.
21. I.D. Zartsyn, A.V. Vvedenskii and I.K. Marshakov, *Russ. J. Electrochem.* **30**(4) (1994) 492.
22. L.M. Kefeli, *Kinet. Katal.* **12**(6) (1971) 1514.
23. A.J. Smith, P. Munroe, T. Tran and M.S. Wainwright, *J. Mater. Sci.* (submitted 1999).